An Omnidirectional Stereo Vision System Using a Single Camera

Sooyeong Yi[*] and Narendra Ahuja[**]
[*]*Div. of Electronics and Information Engineering, Chonbuk National University, Korea*
[**]*Dept. of Electrical and Computer Engineering, Univ. of Illinois at Urbana-Champaign, USA*
[*]*suylee@chonbuk.ac.kr*, [**]*ahuja@vision.ai.uiuc.edu*

Abstract

We describe a new omnidirectional stereo imaging system that uses a concave lens and a convex mirror to produce a stereo pair of images on the sensor of a conventional camera. The light incident from a scene point is split and directed to the camera in two parts. One part reaches camera directly after reflection from the convex mirror and forms a single-viewpoint omnidirectional image. The second part is formed by passing a subbeam of the reflected light from the mirror through a concave lens and forms a displaced single viewpoint image where the disparity depends on the depth of the scene point. A closed-form expression for depth is derived. Since the optical components used are simple and commercially available, the resulting system is compact and inexpensive. This, and the simplicity of the required image processing algorithms, make the proposed system attractive for real-time applications, such as autonomous navigation and object manipulation. The experimental prototype we have built is described.

1. Introduction

The wide field of view (FOV) offered by omnidirectional vision systems make them useful in many application areas. A common approach to omnidirectional image acquisition with a 360^o FOV is catadioptric imaging wherein mirrors are used to map the large field of view onto one or more image sensors. In one such family of methods, a convex mirror is placed in front of a conventional camera. Several types of convex mirrors can be used such as conical, spherical, parabolic, or hyperbolic mirrors [1, 2]. In these methods, the resolution is non-uniform and degrades monotonically away from the direction of viewing. In another family of methods, multiple mirrors are used to map adjacent parts of a large FOV onto multiple sensors [3, 4,18], which results in uniform, higher resolution throughout the FOV. A compromise solution achieves high resolution with a single rotating camera [5], imaging different parts of the FOV sequentially, thus sacrificing the video rate imaging capability of the above families but achieving high resolution.

For omnidirectional stereo vision, an obvious method is to use two (or more) cameras instead of each conventional camera [6]. However, the cameras must be calibrated for various imaging parameters such as focal length, gain, and spectral response [7]. The work on single-camera stereo systems is aimed at avoiding these problems. One straightforward such method uses temporal stereo, i.e., stereo images are acquired sequentially by a single moving camera, e.g. located on a mobile robot. However, depth estimation inaccuracies arise due to uncertainties in the sequential robot/camera positions. Also, depth estimation is not real-time.

As one way of real-time imaging, optical devices such as two planar mirrors with different view angles [7] or a biprism [8] are introduced to split the incoming light into two parts to achieve two different viewpoints simultaneously. Alternatively, multiple omnidirectional imaging systems can be used directly. An example is the use of two-camera stereo with two convex mirrors in [9, 10]. Koyasu *et al.* developed an omnidirectional stereo vision system with two pairs of cameras and convex mirrors for map-making and autonomous navigation of a mobile robot [11]. Basu and Southwell proposed a double-lobed mirror based single camera stereo vision system [12], and developed the associated stereo processing algorithm [13]. Cabral *et al.* also designed a similar double lobed hyperbolic mirror for single camera omnidirectional stereo [14]. Recently, another single camera approach using two pieces of hyperbolic mirrors with a large vertical baseline to improve the accuracy of depth estimates has been reported [15]. The main advantages of the single camera omnidirectional stereo vision systems are the reduced system complexity and simpler image processing algorithms due to reduced need for camera calibration.

A major aim of this paper is to propose a new

0-7695-2521-0/06/$20.00 (c) 2006 IEEE

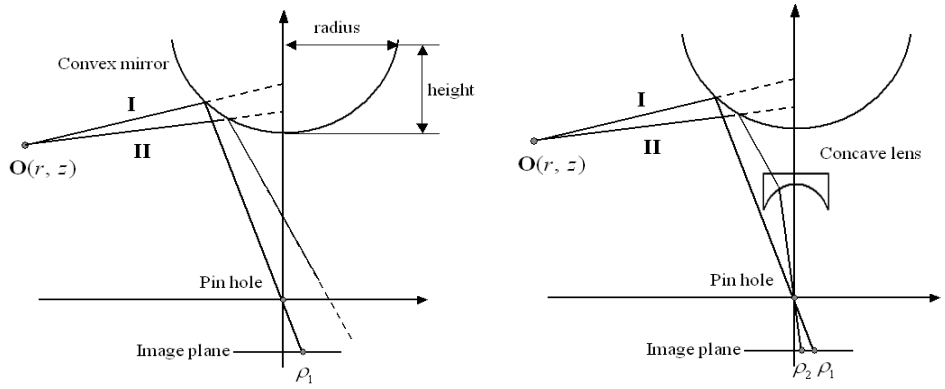

(a) Monocular omnidirectional imaging (b) Omnidirectional stereo imaging with concave
Fig. 1: The proposed single camera omnidirectional stereo vision system.

omnidirectional single camera stereo system which reduces the complexity involved in designing specialized mirrors such as the double lobed mirror or two pieces of hyperbolic mirrors. Our method uses a simple combination of off-the-shelf convex mirrors and a concave lens, yielding a compact and cost-effective solution. In Sec. 2, the principles of the proposed omnidirectional stereo system are briefly described. In Sec. 3, a closed-form depth estimate is provided based on the simple optics for a convex mirror and a concave lens. A prototype of the proposed system and some preliminary experiments with the prototype are described in Sec. 4. Sec. 5 presents concluding remarks.

2. Proposed omnidirectional stereo system

The optical part of the proposed omnidirectional stereo system consists of a convex mirror and a concave lens. The convex mirror shape used is hyperbolic. However, a parabolic mirror could also be used instead.

Fig. 1 illustrates the principles of the proposed system. $\mathbf{O}(r, z)$ denotes an object point. Light ray I from the object is reflected on the hyperbolic mirror, and the reflected ray passes through the pinhole. There is an image point on the sensor plane corresponding to the ray I as shown in Fig. 1 (a). The real object emits the light rays in all directions, not only the ray I of course. However, the other light rays having different directions from ray I, e.g., ray II in Fig. 1 (a), cannot reach the pinhole after reflection, and therefore do not contribute to the image on the sensor plane.

On the contrary, the reflected ray II in Fig. 1 (b) can reach the pinhole owing to refraction through the concave lens. The amount of refraction depends on the refraction index of the lens material, the position, thickness and curvature of the concave lens; and, of course, the incident direction of the ray at the lens which in turn depends on the depth of the scene point. Since both rays I and II come from the same object point, image points ρ_1 and ρ_2 form a stereo pair, which can be used for depth estimation.

3. Depth computation

3.1. Refraction through a concave lens

While passing through the concave lens, a light ray experiences the refraction illustrated in Fig. 2, which is given by Snell's law [17]. First order optics with Gaussian approximation gives the relationships between the incident ray and the refracted ray as follows:

$$p_2'' = p_2 - \frac{p_2 \cdot c}{p_2(n-1)+c} + d - \frac{d}{n} \qquad (1)$$

$$\theta_2'' = \frac{c+(n-1)\cdot p_2}{c} \cdot \theta_2 \qquad (2)$$

where θ_2'' and p_2'' denote the incidence angle and the cross point with the vertical axis, and θ_2 and p_2 represent the angle of the refracted ray and the lens position (Fig. 2). In the sequel, we assume that the origin of the coordinate system is at the pinhole.

In (1) and (2), c , d and n denote curvature, thickness, and the refraction index of the lens material respectively. Here, a plano-concave lens is used without loss of generality; it is also possible to get similar expressions for a biconcave lens.

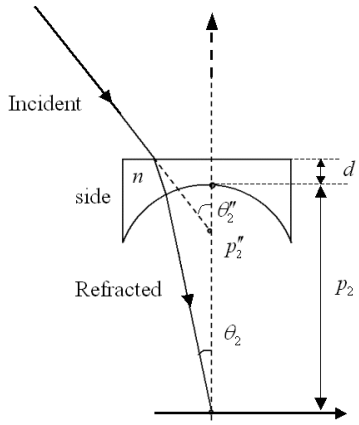

Fig. 2: Refraction through a concave lens.

3.2. Reflection from the hyperbolic mirror

The analysis in this paper is described on the $r-z$ plane rather than in the whole 3D space. It is easy to extend this analysis to 3D space by rotating about the vertical ($\mathbf{z}$) axis. Given the reflected ray with angle θ and cross point p as shown in Fig. 3, it is possible to obtain the equation for the incident ray from an object point, $\mathbf{O}(r, z)$, based on the simple reflection law. The hyperbolic curve, $M(r)$, with focal point at h, can be represented on $r-z$ plane using

$$\frac{(z-h+f)^2}{a^2}-\frac{r^2}{b^2}=1 \quad \equiv \quad z=M(r)=h-f+\frac{a}{b}\sqrt{r^2+b^2} \tag{3}$$

where a and b denote the parameters of the hyperbolic function, and f represents its focal point given by

$$f=\sqrt{a^2+b^2} \tag{4}$$

The reflected ray is then described by the given angle θ and the cross point p as:

$$z=-\cot\theta\cdot r+p \tag{5}$$

The intersection point $\mathbf{C}$ of the hyperbolic function (3) and the reflected ray (5) is denoted as $\mathbf{C}(r_c, z_c)$. Then, the incident ray from an object $\mathbf{O}(r, z)$ can be parameterized as:

$$z=\cot\phi\cdot r+z_o \tag{6}$$

where ϕ and z_o represent vertical angle and cross point with $\mathbf{z}$ axis as shown in Fig. 3.

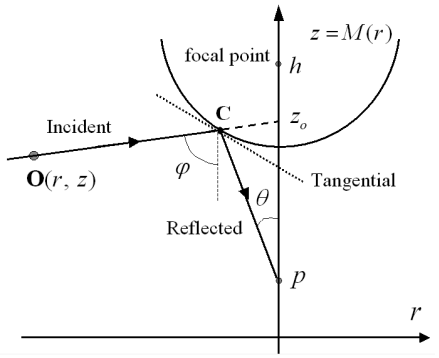

Fig. 3: Reflection on a hyperbolic mirror.

By using the simple law of reflection on a specular surface and the geometry given in Fig. 3, it is possible to get the first parameter, ϕ in (6) as follows:

$$\phi=\theta+2\cdot\tan^{-1}\left(\left.\frac{dM(z)}{dr}\right|_{\mathbf{C}}\right) \tag{7}$$

$$\left.\frac{dM(z)}{dr}\right|_{\mathbf{C}}=\frac{a^2}{b^2}\cdot\frac{r_c}{z_c-h+f} \tag{8}$$

Since the incident ray (6) should pass through $\mathbf{C}(r_c, z_c)$, the parameter z_o, can be represented by:

$$z_o=z_c-\cot\phi\cdot r_c \tag{9}$$

In other words, given angle θ and cross point p of the reflected ray, the corresponding incident ray toward z_o is described by (6), where the parameters, ϕ and z_o can be obtained from (7-9).

It is assumed in this paper that the first focal point of the hyperbolic mirror is located at $h=2f$, so that the pinhole position of a camera coincides with the second focal point of the hyperbolic mirror. According to the property of the hyperbolic function, all incident rays toward the first focal point, i.e., $z_o=2f$, reach the pinhole at the origin after reflection. Thus, the reflected ray always has $p=0$ without regard to θ.

3.3. Depth computation

As shown in Fig. 4, the position of the object point, $\mathbf{O}(r, z)$ is the solution of the simultaneous equations for rays **I** and **II**. Thus, it is necessary to get the expressions for the rays based on the measurement data in the system. Given ρ_1 and ρ_2 on the image plane in

Fig. 4, the vertical angles of two rays toward the pinhole are described by

$$\theta_1 = \tan^{-1}\left(\frac{\rho_1}{\lambda}\right) \quad (10\text{-}1)$$

$$\theta_2 = \tan^{-1}\left(\frac{\rho_2}{\lambda}\right) \quad (10\text{-}2)$$

where λ denotes the distance from the pinhole to the image plane.

The equation for ray **I** in Fig. 4 can be obtained as follows. Recall that only the incident ray toward the first focal point can reach the pinhole after reflection from the hyperbolic mirror. Thus the other parameter, z_o for ray (6) becomes $z_o = 2f$. The parameter, ϕ in (6) is obtained by inserting the measurement (10-1) into (7) together with (8). Ray **I** satisfies

$$z = \cot\phi_1 \cdot r + 2f \quad (11)$$

In order to get the equation for ray **II** , refraction through the concave lens should be taken into consideration. As described in Sec. 3.1, it is possible to get θ_2'' and p_2'' by (1) and (2), given θ_2 and p_2 , where p_2 denotes known position of the concave lens. Again, by inserting θ_2'' and p_2'' into (7-9), it is possible to get ϕ_2 and z_{o2} to obtain ray equation

$$z = \cot\phi_2 \cdot r + z_{o2} \quad (12)$$

Detailed expressions for the parameters are omitted here for brevity. The solution of the simultaneous equations (11-12) gives the object point $\mathbf{O}(r, z)$:

$$\begin{bmatrix} r \\ z \end{bmatrix} = \begin{bmatrix} \cot\varphi_1 & -1 \\ \cot\varphi_2 & -1 \end{bmatrix}^{-1} \cdot \begin{bmatrix} -2f \\ -z_{o2} \end{bmatrix} \quad (13)$$

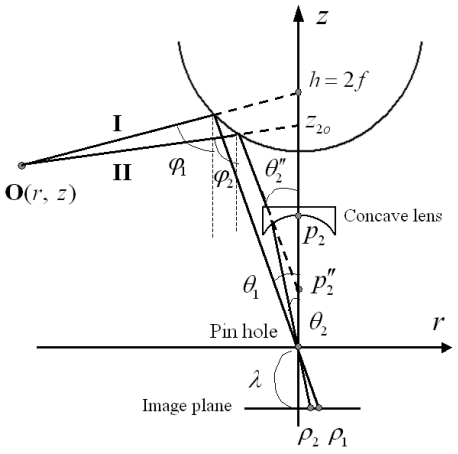

Fig. 4: Depth computation given stereo pair

4. Experimental results

A prototype of the proposed was built (Fig. 5) which has parameters given in Table 1. The omnidirectional stereo images acquired by the proposed system, and the corresponding omnidirectional images are presented in Fig. 6(a) and 6(b) respectively. As shown in Fig. 4, the side of the concave lens blocks the light rays in some vertical angles, which causes the opaque ring at the boundary between the outer and the inner stereo images as shown in Fig. 6. By slanting the lens side off vertical, it is possible to minimize the blocked angle, and thereby, the thickness of the opaque ring in the image. In the orthographic imaging system with a parabolic mirror on the other hand, the vertical side of the lens is preferable over the inclined side.

Since the epipolar lines are collinear in the radial direction in the omnidirectional stereo image, stereo matching is relatively easy. Recently, many algorithms for matching omnidirectional stereo images have been developed [13, 15, 16].

Table 1 Parameters of the experimental system

(a) Mirror (all in mm)

Parameter	*a*	*b*	*f*	radius	height
Value	28.095	23.4125	36.57	30.0	20

(b) Concave lens

Parameter	*n*	*d*	*c*	p_2	radius
Value	1.7	2 mm	58.8 mm	52 mm	15 mm

(c) Camera

Parameter	focal length	resolution
Value	2.7 ~ 8 mm	1/3", 1024x768

Fig. 5: Prototype

5. Conclusion

Past approaches to omnidirectional stereo imaging with a single camera use (1) a double lobed mirror [13, 14] or (2) two mirrors [15] We have described a third approach that (3) uses a mirror and a concave lens. The optical part consists of a convex mirror and a concave lens. By adjusting the position of the concave lens, it is possible to control the stereo disparity and thus the accuracy of the 3D distance computation. Since the optical components used are commercially available, the proposed design is compact and cost-effective. We have derived a closed-form relationship involving 3D distance. The proposed method is versatile in that it is also applicable to different types of convex mirrors, e.g., the parabolic mirror. (2) involves a relatively lengthy baseline, and thus longer range of sight than (1) and (3). Two simple ways of increasing range of sight with (1) and (3) are to use a larger mirror or a camera with higher resolution.

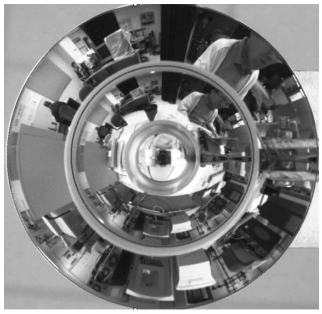

(a) Omnidirectional image

(b) Panoramic image

Fig. 6: Experimental Image

Acknowledgement

The support of the National Science Foundation under grant NSF IBN 04-22073 is gratefully acknowledged.

6. References

[1] S. Baker and S. Nayar, "A theory of Single-Viewpoint Catadioptric Image Formation," *Int'l Journ. of Computer Vision*, vol. 35, no. 2, pp 175-196, 1999.

[2] S. Nayar, "Catadioptric Omnidirectional Camera," *Proc. of IEEE Conf. on Computer Vision and Pattern Recognition*, pp.4820488, 1997.

[3] V. Nalwa, "A true omnidirectional viewer," *Bell Lab. Tech. Report*, 1996

[4] H. Hua and N. Ahuja, "A High-Resolution Panoramic Camera," *Proc. of IEEE Conf. on Computer Vision and Pattern Recognition*, pp. 960-967, 2001.

[5] A. Krishnan and N. Ahuja, "Range Estimation from Focus Using a Nonfrontal Imaging Camera", *Int'l. Jour. of Computer Vision*, vol. 20, no. 3, pp. 169-185, 1996

[6] K. Tan, H. Hua and N. Ahuja, "Multiview Panoramic Cameras Using Mirror Pyramids", *IEEE Tr. on Pattern Analysis and Machine Intelligence*, vol. 26, no. 6, 2004

[7] J. Gluckman and S. Nayar, "Catadioptric Stereo Using Planar Mirrors", *Int'l Journ. of Computer Vision*, vol. 65-79, 2001.

[8] D. Lee and I. Kweon, "A novel stereo camera system by a bi-prism," *IEEE Tr. on Robotics and Automation*, vol. 16, no. 5, pp. 528-541, 2000.

[9] J. Gluckman, S. Nayar and K. Thorek, "Real-time omnidirectional and panoramic stereo," *Proc of DARPA Image Understanding Workshop'98*, vol. 1, pp. 299-303, 1998

[10] T. Pajdlar, T. Svobda and V. Hlavac, "Epipolar geometry of central catadioptric camera," *Int'l Jour. of Computer Vision*, vol. 49, no. 1, pp. 23-37, 2002.

[11] H. Koyasu, J. Miura and Y. Shirai, "Recognizing moving obstacles for robot navigation using real-time omnidirectional stereo vision," *Journ. of Robotics and Mechatronics,* vol. 14, no. 2, pp. 147-156, 2002.

[12] D. Southwell, A. Basu, M. Fiala and J. Reyda, "Panoramic Stereo," *Proc. of ICPR'96*, pp. 378-382, 1996.

[13] M. Fiala and A. Basu, "Panoramic stereo reconstruction using non-SVP optics," *Computer Vision and Image Understanding*, vol. 98, pp. 363-397, 2005.

[14] E. Cabral, J. Souza and C. Hunoid, "Omnidirectional Stereo Vision with a Hyperbolic Double Lobed Mirror," *Proc. of Int'l Conf. on Pattern Recognition'04*, pp. 1-4, 2004.

[15] G. Jang, S. Kim and I. Kweon, "Single Camera Catadioptric Stereo System," *Proc. of Workshop on Omnidirectional Vision, Camera Networks and Non-classical cameras(OMNIVIS2005),* 2005

[16] Z. Zhu, "Omnidirectional Stereo Vision," *Proc. of ICAR'01*, pp. 22-25, 2001.

[17] F. Jenkins and H. White, *Fundamentals of Optics*, 4th ed. McGraw-Hill, 1976

[18] http://vision.ai.uiuc.edu